

## Assessing Electronic Devices with Advanced 3D X-Ray Imaging and Electron Microscopy

Herminso Villarraga-Gómez, Ph.D., Kyle Crosby, Ph.D.  
Carl Zeiss Industrial Quality Solutions, LLC  
herminso.gomez@zeiss.com; kyle.crosby@zeiss.com

### ABSTRACT

This article presents advanced workflows that combine 3D X-ray microscopy (XRM), nanoscale tomography, and electron microscopy to generate detailed visualization of the interior of electronic devices and assemblies to enable the study of internal components for failure analysis (FA). Recently developed techniques such as integrating deep learning (DL)-based algorithms for 3D image reconstruction are also discussed in this article. Additionally, a DL-based tool (called DeepScout) is introduced that uses high-resolution 3D XRM datasets as training data for lower resolution, higher field of view datasets and scales larger volume data using a neural network. Ultimately, these workflows can be performed independently or complementary to other multiscale correlative microscopy assessments and will provide valuable insights into the internal workings of electronic packages and integrated circuits across multiple length scales, from macroscopic features on electronic devices (e.g., hundreds of mm) to microscopic details in electronic components (in the order of tens of nm). Understanding advanced electronic systems through X-ray imaging and electron microscopy, possibly integrated with additional correlative microscopy investigations, can accelerate development time, increase cost efficiency, and simplify FA and quality inspection of electronic packaging, printed circuit boards (PCBs) and electronic devices assembled with new emerging technologies.

Key words: X-ray microscopy, failure analysis, deep-learning, nanoscale tomography, electron microscopy.

### INTRODUCTION

Several X-ray based technologies began in medicine, then found use in industrial applications, and are today widely used in assembly analysis of manufactured medical devices, electronics, semiconductor packages, printed circuit boards, etc. [1, 2, 3]. Some of the techniques that can be used for NDT include radiography, laminography, limited angle tomography, and computed tomography; they can be of assistance in the determination of voids/porosity, flaws, cracks, and fault insulation within assembled parts from the electronics industry. Different degrees of packages from light-emitting diodes, hybrids, power devices, multi-layer wire-bonded packages to ultra-fine pitch devices can be inspected for package requirements or defective behaviors. Fully populated PCBs are typically inspected to characterize voids in the packages, solder bridges, pad alignments, etc., and to look for traces of failure such as wire sweeps, solder defects, cracking, undersize or oversize elements, and missing components. System-in-package (SiP) technologies can resemble PCBs in miniature,

through their use of heterogeneous integration to deliver high performance in a smaller form factor than a traditional PCB. SiP may use chips of different silicon nodes and combine legacy interconnects such as wire bonds with the latest interconnect technology such as hybrid bonds, Cu-pillar microbumps, or redistribution layers (RDL) with fine pitch approaching 1 micron or less.

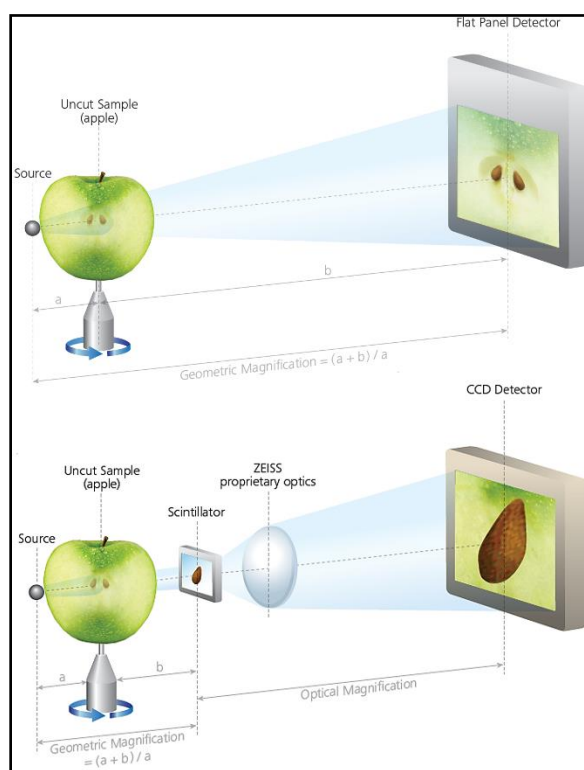


**Figure 1.** Schematic representation of a general X-ray CT setup with a flat panel detector (top) and the two-stage magnification architecture (bottom) of a 3D X-ray microscope with optical magnification. Combination of geometric and optical magnification enables higher resolution capabilities in XRM as compared to flat panel X-ray CT systems.

Although 2D radiographic imaging and/or computed laminography can still extract valuable information when there are some overlapping materials and obstructed components, they still have limitations that can be challenging for advanced packages. Radiographic projections cannot discern depth and laminography has a limited depth resolution, so a more comprehensive analysis of a device would need advanced X-ray technologies such as computed tomography (CT) or 3D XRM. As the global electronic industry continues to grow and

require top tier safety and quality standards, advanced NDT technologies are needed for FA to meet those demands. In this article, the authors discuss modern 3D X-ray based approaches that connect sub-micrometer, nanoscale X-ray imaging for assessing semiconductor packaging and electronic devices, describing how these different methods have practical application and how to link them to other imaging techniques used in the electronics industry, e.g., electron microscopy.

### 3D X-RAY IMAGING & ELECTRONIC INSPECTION

Assembly analysis, structural characterization, and fault isolation provide critical information for improving product development and manufacturing processes in the electronics industry. For increasing the confidence of FA assessments, one alternative is to perform 3D X-ray imaging, e.g., CT. In traditional industrial X-ray systems, the main approach has been to use projection-based architectures in which 2D images are created by the projection of divergent X-ray beams passing through an object and producing radiographs on a flat-panel detector (Figure 1, left). A CT processing algorithm can create a virtual 3D volume reconstruction of the object from multiple radiographic images, collected at different angular positions as the object is rotated by certain angular increments, typically covering 180 or 360 degrees. From the reconstructed volume, internal and external features can be extracted to reveal the object's 3D structure and morphology [3, 4, 5]. However, in traditional flat panel-based X-ray systems using simple geometric magnification, which is determined by the size of the sample and the working distance from the X-ray source and detector, the spatial resolution requirements to scan small electronic features inside electronic components tend to limit the size of the sample that can be scanned. Such a limitation can be overcome with the use of 3D X-ray XRM that use geometric and optical magnification with "resolution-at-a-distance (RaaD)", e.g., see Figure 1 (right) or Refs. [6, 7]. In X-ray CT, the resolution of the system worsens as the geometrical magnification decreases (i.e., when the sample size increases). On the other hand, the advantage of optical magnification allows XRM to preserve and deliver improved spatial resolution as the optical magnification increases. This is possible without major limitations on sample size, when RaaD capabilities are introduced in the XRM system design and as long as the sample physically fits inside the instrument.

As interconnect dimensions shrink in advanced packaging architectures, making the thickness and volume of each layer smaller, it is difficult to obtain high-contrast images with conventional absorption/contrast X-ray imaging, especially at nanometer length scales. Microbump interconnections for 3D integration are projected to scale to 5  $\mu\text{m}$  pitch and the back-end-of-line (BEOL) process of semiconductor fabrication has increased in complexity [1]. Failures related to chip-package interaction resulting from fabrication and assembly stresses can have structural dimensions below 1  $\mu\text{m}$ .

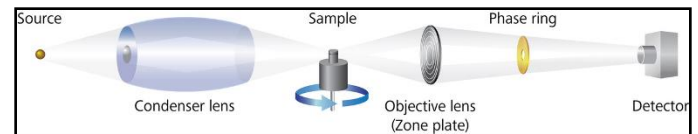


**Figure 2.** Schematic representation of a nanometer-resolution 3D X-ray microscope, which uses a Fresnel zone plate to form a magnified image of the sample in the detector. The outermost ring of the zone plate determines the spatial resolution of the microscope. An optional phase ring can be inserted into the beam path to achieve Zernike phase contrast to visualize features in low absorption samples.

These small dimensions require microscopy instruments with increased capabilities in terms of spatial resolution and image quality. Fortunately, there are ways to improve the contrast and resolution of XRM into the nanometer range, e.g., by using X-ray focusing elements such as Fresnel zone plates or Kirkpatrick-Baez mirrors [8, 9, 10, 11], though the field of view is considerably reduced and may require sample preparation to isolate a small volume from the bulk package. Although in such a case the X-ray inspection requires sample preparation, it is considered non-invasive as it preserves the region of interest, e.g., where there may be a defect, intact. This allows subsequent analysis by other methods after the XRM scan. The optical schematics of the nanometer-resolution 3D XRM is shown in Figure 2, in which a high-brightness X-ray source is focused on a sample by a capillary condenser lens. The purpose of the condenser lens is to provide uniform illumination of the sample throughout the field of view. A Fresnel zone plate objective then forms a magnified image of the sample in the X-ray camera (detector). As the sample is rotated, images are collected at a variety of projection angles which are then reconstructed into a 3D tomographic dataset.

### XRM WORKFLOWS FOR ELECTRONIC DEVICES

Due to the non-destructive nature of 3D XRM imaging, the interior arrangements of electronic devices can be imaged without disassembly. This allows engineers and researchers to observe the arrangement of internal features of intact electronic components, such as PCBs, to evaluate their structural integrity and check for the existence of defects or identify the root cause of failures. An example of a typical 3D XRM imaging workflow for assessing electronic devices is shown in Figure 3, which shows images from a smartphone scanned with a 3D XRM instrument. A flat-panel detector was used to scan the full device. Then, by using the optical lenses of the 3D XRM to increase magnification levels, small regions of interest in the device were scanned at high resolution. For example, the circuit board or micro-processor inside the smartphone was scanned to see if there are any defects in the surface-mount packaging or porosity inside the solder joints (BGA balls) that may affect the functional performance of the device. By increasing the optical magnification, details in the microprocessor such as the arrangement of BGA packages and the vias that connect different layers in the device can be observed at high-spatial resolution (Figure 4). Using the same principle, other regions of interest can be explored in the device, e.g., assembly inspection of camera lens modules. When smartphone camera lens modules are in the assembled state, the evaluation of the

geometric properties of the lenses, such as the thickness of the annular wedges, the centering interlock diameters, the spaces between the wedges, the lens-to-lens tilt, the vertex heights, and centration, etc., require a non-contact and non-destructive measurement method such as 3D XRM [6].

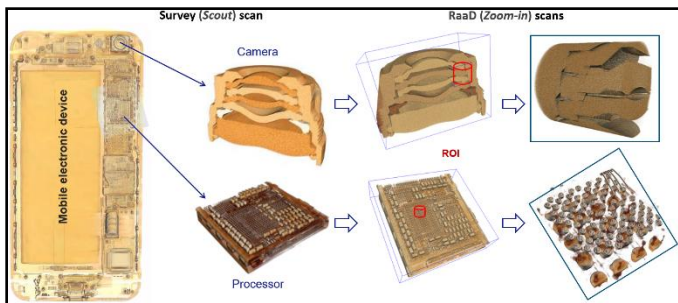


**Figure 3.** By using a 3D X-ray microscope, featuring resolution-at-a-distance (RaaD) capabilities through a set of different magnification lenses [2], fine details in different regions of interest (ROIs) can be imaged in an electronic device without disassembling the sample.

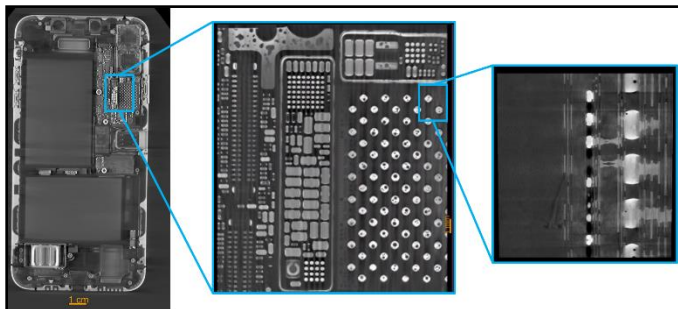


**Figure 4.** Visualization of cross-sectional images of the interior of a smartphone illustrating fine details, e.g., BGA voids and through-hole vias in the microprocessor, in small regions zoomed in with a 3D X-ray microscope with RaaD capabilities.

### XRM WORKFLOWS FOR ASSESSING PCBs

The main workflow for assessing electronic devices and their components using 3D XRM with RaaD capabilities is illustrated in Figure 5 and can be summarized in three steps: (1) an operator selects the settings for scanning the sample based on its geometry, size, and composition; (2) the XRM instrument rotates the sample while the detector collects snapshots or radiographic projections at different angular positions; and (3) using the 2D radiographic projection data, a software reconstruction will generate a 3D volumetric density map of the sample that reveals its internal and external features. The 3D reconstructed volume can be used for non-destructive inspection using cross-sectional views or 2D slices to see through the inside of the sample—virtually, without physically cutting or destroying it. However, the uneven penetration of X-rays into flat (high-aspect-ratio) samples, such as PCBs or IC packages, can lead to CT reconstruction artifacts, e.g., cupping and streaks, that affect the voxel values in the reconstructed image and make the quantitative evaluation of small features challenging. Such limitations are overcome with the use of a high-aspect-ratio tomography (HART) scan modality, which collect fewer projections along the broad side of a flat sample

and more along the thin side, to optimize image quality and spatial resolution around the edges of the long sample side. The principle of HART operation is illustrated in Figure 6 along with an application example for scanning a smartwatch and the SiP contained within it.

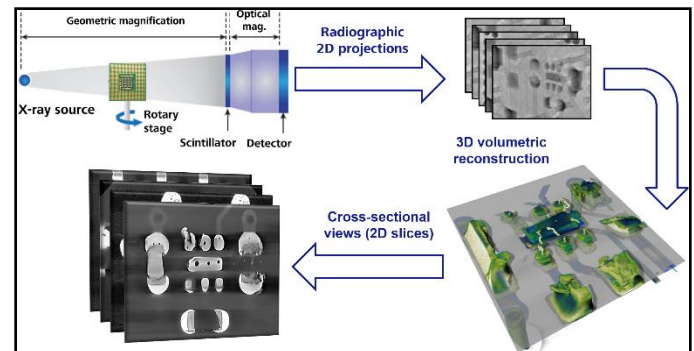


**Figure 5.** Workflow for 3D X-ray microscopy measurement. False colors can be added after volumetric reconstruction to segment the object (e.g., electronic circuit board) into its different components. Cross-sectional (2D slice) images can be used to inspect the object’s internal features.

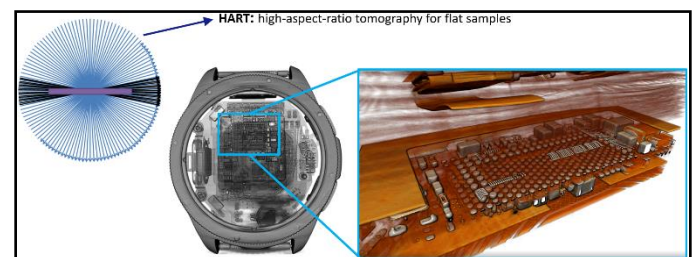


**Figure 6.** In the HART scan modality, the radiographic projection spacing is manipulated as the sample rotates, thus optimizing data density [2]. A wealth of data is provided by closely spaced long X-ray views versus less densely spaced short views, maximizing information of image acquisition. Application examples of HART include the scanning of the SiP present inside electronic devices such as smartwatches.

Although direct radiography is still widely used as an X-ray inspection technique of electronic components to acquire real-time projection images of the internal structures of an object, the problem of single radiographic projections is that there can be detection limitations by their two-dimensional nature and the superimposition of several radiographic shadows coming from multiple components that can have different X-ray absorption coefficients, and which can be located at different planes inside a specimen. It may be challenging to visualize a void or other defects from direct inspection of a radiographic image due to superimposed structures with different material density. This problem is eliminated through 3D tomographic reconstruction with the extraction of different cross-sectional views or 2D slices from 3D reconstructed CT data, e.g., see Figure 7. Aided by the volumetric data generated by 3D XRM with RaaD, several types of defects can be explored in a non-destructive manner, e.g., voids in solder bumps, underfills, fatigue cracks, cold joints known as “head-on-pillow”, trace cracks or breaks, electromigration, broken vias, microbump shorts, solder bleeds,

cracks or micro-cracks in silicon wafers, etc.

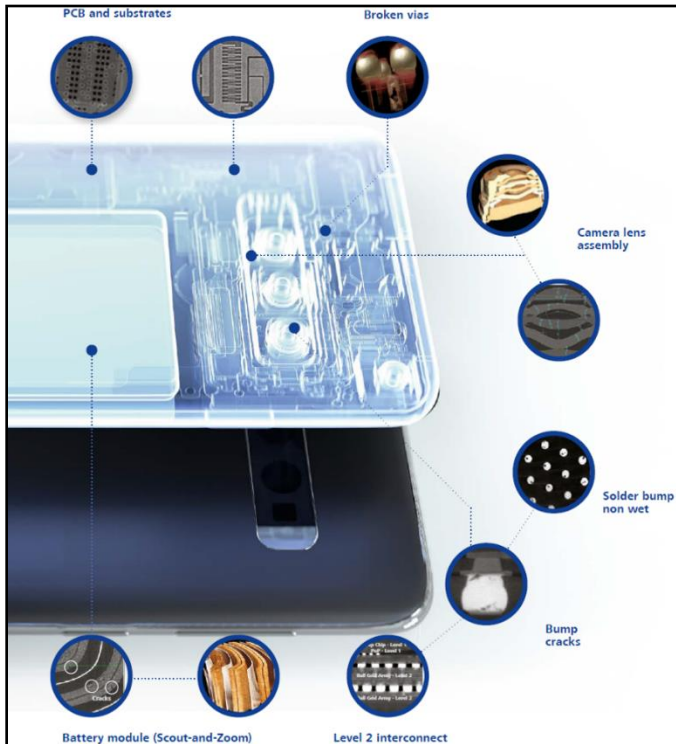


**Figure 7.** Different types of defects within electronic devices can be explored with the use of a 3D X-ray microscopy.

### CORRELATIVE FA WORKFLOWS

Current innovations in semiconductor packaging enable SiP and heterogeneous integration of advanced electronic components using silicon chips and designs that include through-silicon vias and chiplets containing hybrid bonding. Characterization and failure analysis of these advanced technologies are essential to the overall development and delivery of reliable, high-performance products. Small features, e.g., through-silicon vias and microbumps, may be embedded between layers or non-uniformly staggered/distributed along the sides. It is difficult to perform defect recognition and failure analysis of these features with conventional 2D X-ray inspection or computed laminography. These challenges can be overcome with FA workflows that combine 3D XRM (with RaaD capabilities) and nanoscale tomography, e.g., see Figure 8 and Figure 9. As seen from Figure 8 and Figure 9, correlative FA workflows may start with non-destructive approaches for failure confirmation, e.g., standard 3D X-ray imaging, and then progress to more destructive analyses that require some sort of sample preparation for mechanical isolation of a region of interest in an electronic package. To prevent altering potential areas where a defect of interest may be, i.e., to avoid inducing cracks, delaminations, or other artifacts generated by physical cross-sectioning of the sample, nanoscale 3D X-ray imaging can be used after fault isolation for a non-invasive exploration. After that, further investigation can be performed with the use of nanoprobing or any other advanced FA techniques that may require cross-sectional sample preparation such as scanning electron microscopy (SEM), transmission electron microscopy (TEM), atomic force microscopy (AFM), energy dispersive

spectroscopy (EDS), or secondary-ion mass spectrometry (SIMS), e.g., see Figure 9 and Figure 10. Since physical sectioning techniques provide only information from a single cross-sectional plane, the addition of 3D X-ray imaging to FA workflows is essential to accurately determine defect location prior to cutting or opening a device. In some cases, the root cause of a failure can even be identified from 3D XRM data without the need for additional inspection.

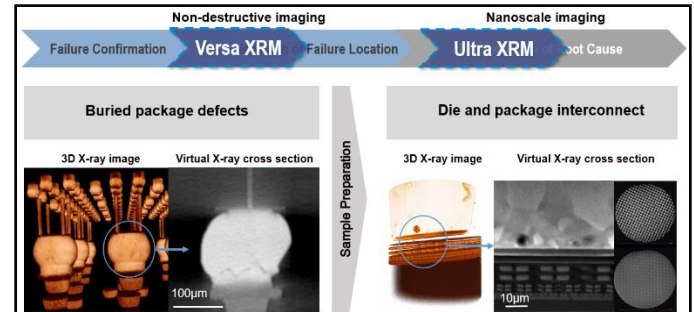


**Figure 8.** Package FA workflow combining sub-micrometer and nanoscale 3D X-ray microscopy imaging on a small region of interest [2]. RaaD enables CT reconstructions of the microstructure inside electronic components, at high spatial resolutions, without slicing the sample.

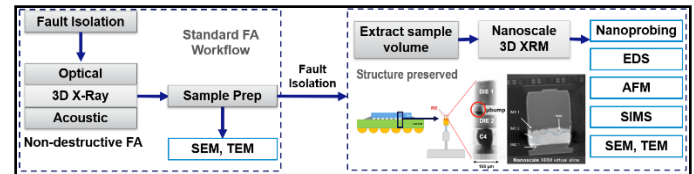


**Figure 9.** An expanded workflow for fault insulation and FA in advanced electronic packages [2], which includes nanoscale 3D X-ray microscopy.

As an example of a correlative workflow between 3D XRM and a focused ion beam scanning electron microscope (FIB-SEM) with an integrated femtosecond laser, Figure 10 shows the results of an FA investigation in a semiconductor package [13]. After identifying the geometry and location of a region of interest from the 3D XRM dataset, the sample was loaded into the main chamber of a FIB-SEM tool. Then, SEM images were acquired from the outer contours of the package and registered with the same contours visible in the 3D XRM dataset using the correlative workspace of the tool software. An overlay of a cross-sectional view of the defective solders to an SEM image of the package surface was used to precisely define the laser milling area. The sample was then transferred to the integrated laser processing chamber that is separate from the instrument's main chamber to protect its vacuum and detection system from contamination by ablated materials. A trench of the sample was milled with the laser in 29 minutes. The quality of the laser cross-section was sufficient for SEM overview imaging. An SEM image that correlates to the XRM cross-sectional view is shown in Figure 10.

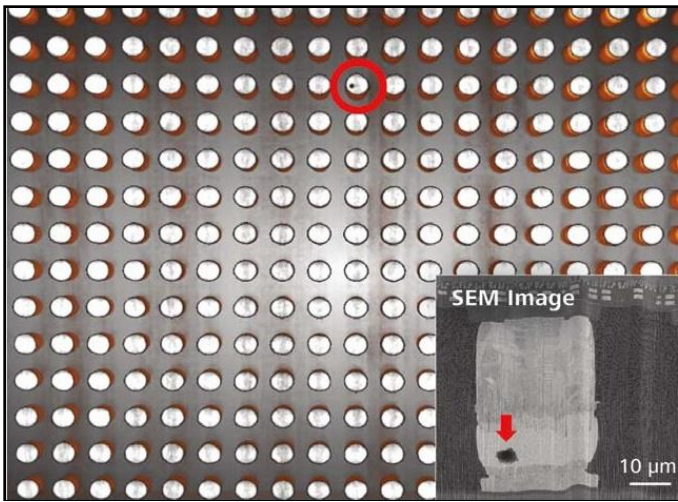


**Figure 10.** Results of a correlative FA investigation in a semiconductor package showing a cross-sectional X-ray microscopic image of a PCB, with a large field of view, and a small SEM image detailing one of the solder bonds defects (a void) after polishing the sample with the FIB.

### USING DEEP LEARNING TECHNIQUES

The integration of deep learning (DL) based algorithms for CT reconstruction was recently introduced into 3D XRM workflows by innovations developed at Carl Zeiss X-ray Microscopy [14, 15]. Data reconstructions produced by DL-based algorithms can provide up to 4x and in some cases even 10x throughput improvement at similar or better image quality compared with the results from standard algorithms such as Feldkamp-Davis-Kress (FDK), e.g., see Figure 11 and Figure 12. Cross-sectional views from the reconstruction of a smartphone camera lens module [12], using a voxel size  $V_x = 7.5 \mu\text{m}$ , are shown in Figure 11. They reveal images of the lens stack reconstructed with different numbers of X-ray projections ( $N_p$ ). It is observed that FDK data reconstructed with  $N_p = 120$  are significantly affected by aliasing artifacts and noise, thus showing the effects of undersampling. By contrast, the DL-based data, still using  $N_p = 120$  ( $t = 9 \text{ min}$ ), shows significantly better contrast-to-noise ratio and these data can enable faster dimensional measurement inspection and assembly verification of cell phone camera lens stacks. This case study demonstrates the effectiveness of using DL-based workflows to reduce the data acquisition time of 3D XRM by a factor of ten, at similar or better image quality compared to standard FDK data reconstructions that require long scans with large  $N_p$  values (in the thousands).

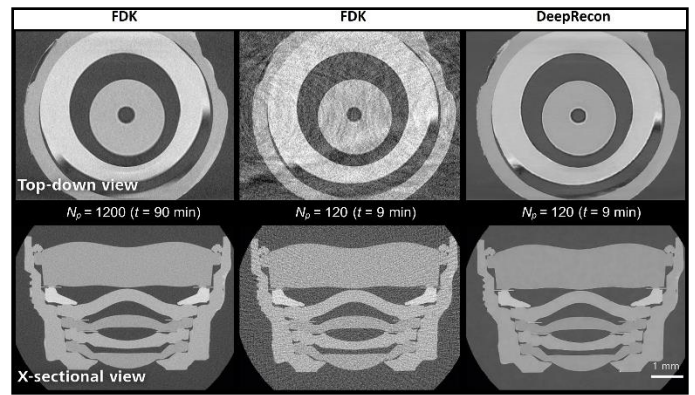


**Figure 11.** X-ray microscopy data for a smartphone camera lens assembly ( $V_x = 7.5 \mu\text{m}$ ) [12]. By using two different cross-sectional views, data reconstructed through FDK with  $N_p = 1200$  ( $t = 90 \text{ min}$ ) are compared with FDK and DeepRecon data that use  $N_p = 120$  ( $t = 9 \text{ min}$ ).

Cross-sectional views from the reconstruction of a 2.5D interposer package, tested by the JEDEC thermal cycle standard, scanned with a 3D XRM instrument using a voxel size  $V_x = 0.7 \mu\text{m}$ , are shown in Figure 12. Features of interest are structural changes of BGA bumps ( $\sim 100 \mu\text{m}$ ) and microbumps ( $\sim 30 \mu\text{m}$ ). DeepRecon produces data with enhanced contrast-to-noise-ratio (CNR), preserving fine details and defining clear boundary separations between air and material, which reveals voids and cracks that get lost in the noise of FDK data reconstructed with  $N_p = 300$ . In addition to improving image quality, the DL-based reconstruction reduces XRM scan time, where data acquisition was reduced by a factor of four with  $N_p = 300$  ( $t = 30 \text{ min}$ ).

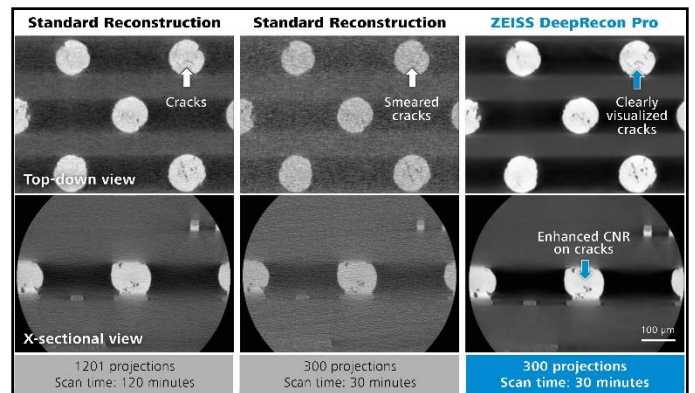


**Figure 12.** XRM data for a BGA from an interposer package ( $V_x = 0.7 \mu\text{m}$ ). Data reconstructed through FDK with  $N_p = 1200$  ( $t = 120 \text{ min}$ ) are compared with FDK and DeepRecon data that use  $N_p = 300$  ( $t = 30 \text{ min}$ ). Features of interest are structural changes in BGA bumps.

Another innovative DL-based reconstruction algorithm to reduce the data acquisition time of 3D XRM is DeepRecon (recently developed at Carl Zeiss X-ray Microscopy), which uses high-resolution 3D XRM datasets as training data for lower resolution, larger field of view datasets and upscales the larger volume data using a neural network model. DeepScout was developed through continued algorithmic innovation enabled by the artificial intelligence. It employs a unique scout-

and-zoom capability to acquire richer information at higher resolution, including interior XRM tomographies for large samples. At its core, DeepScout relies on the ability to generate multiscale, spatially registered datasets and uses that ability to train neural networks to improve the reconstruction. New capabilities, fueled by deep learning, mitigate the traditional trade-off between field of view and resolution. An application example for DeepScout is presented in Figure 13, which shows both low resolution and high resolution XRM data from a section of circuit board, obtained with standard FDK reconstruction methods, and the result from DeepScout reconstruction, in both small and large field of views,

demonstrating how datasets can be upscaled to high-resolution 3D XRM large volume datasets. Thus, DeepScout enables high resolution FA analyses in a large volume of an electronic component with no need for a large quantity of high-resolution scans throughout the device. It only needs one high-resolution scan in a small field-of-view for deep-learning training. The single full field-of-view DeepScout scan was generated in a couple of hours. A single high-resolution scan took 1.5 hours. With standard FDK reconstruction methods it would require at least 9 high-resolution scans, i.e., more than 13 hours, to achieve the same volume and quality of data as the DeepScout scan.

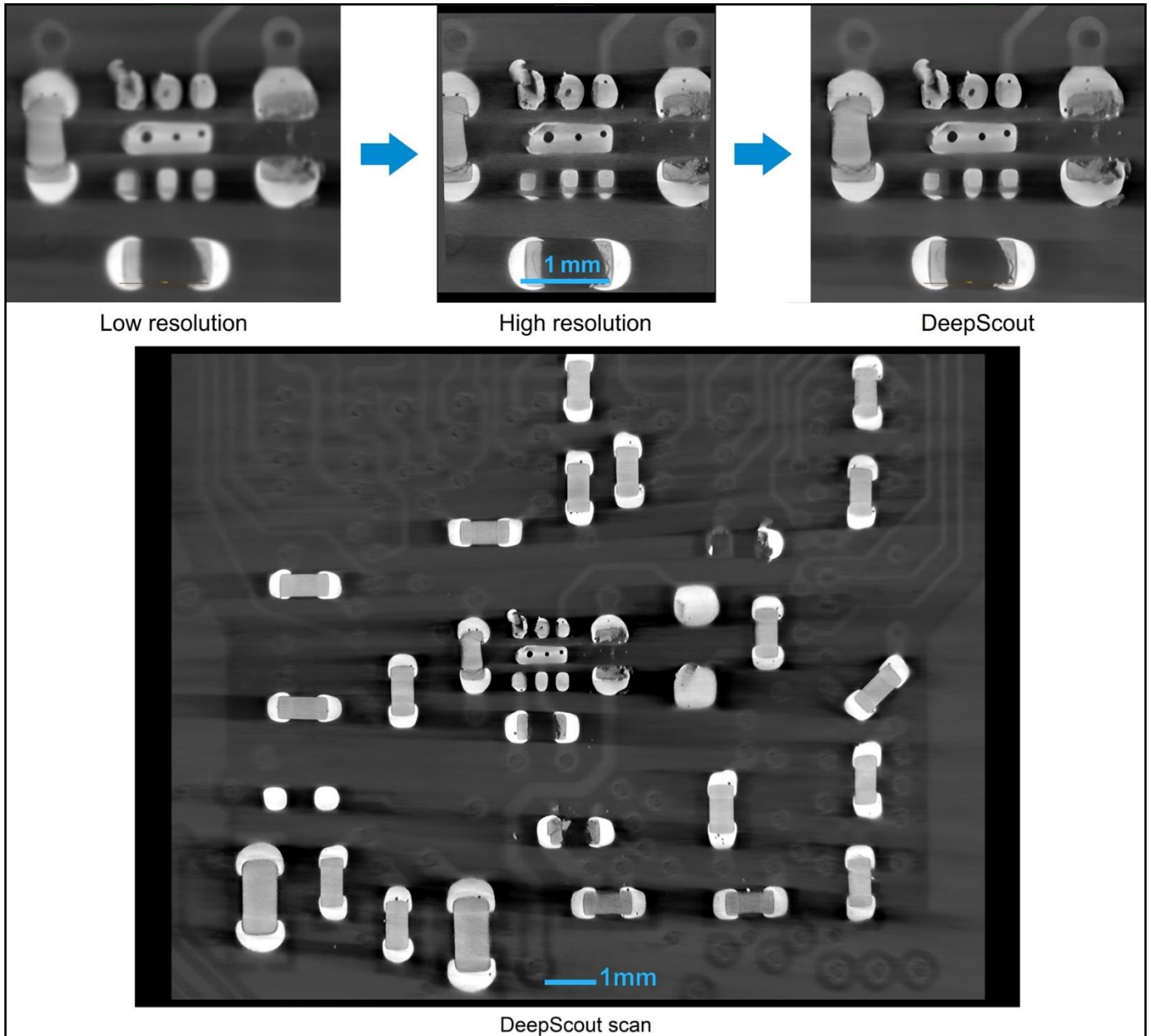


**Figure 13.** Low and high resolution XRM data of a circuit board section, obtained with standard FDK reconstruction, and the result of DeepScout reconstruction, in small and large fields of view, demonstrating how datasets can be scaled to large, high-resolution 3D XRM large volume datasets. A single high-resolution scan took 1.5 hours. The full field-of-view DeepScout scan was generated in a couple of hours, thus reducing the time it would take to perform several high-resolutions scans to be reconstructed with standard FDK methods and achieve the same volume and quality of data.

## CONCLUSIONS

Advances in electronic packaging have led to 3D level integration, an increase in the number of interconnects, and a reduction in solder pitch, volume, and height. This results in increasingly complex packaging architectures, creating new manufacturing challenges and greater risks of failure. Furthermore, because the physical location of faults is often buried within these complex 3D structures, conventional FA methods are becoming less effective. New techniques are needed to isolate and determine the root cause of failures. Recent advances in 3D X-ray imaging enable new FA workflows for electronic devices with the integration of 3D XRM (with RaaD, HART, and DL reconstruction capabilities) and nanoscale tomography. These imaging workflows enable spatially resolved imaging of fine details within electronic devices without interfering with or destroying the root cause of the failure. Due to the multiscale nature of electronic packages, with relevant feature sizes ranging from nanometers to centimeters, the use of correlative imaging workflows that include other imaging methods such as electron microscopy may be useful (e.g., see Figure 9 and Figure 10). Furthermore, using deep learning-based algorithms for CT reconstruction allows the application 3D XRM workflows in a much more cost-effectively way by reducing the time required for data acquisition. DL-based X-ray inspection technologies will have a major impact on the testing and failure analysis of advanced semiconductor packages where non-destructive imaging at sub-micrometer levels of resolution is often required.

## REFERENCES

- [1] C. Hartfield, C. Schmidt, A. Gu and S. T. Kelly, "From PCB to BEOL: 3D X-ray microscopy for advanced semiconductor packaging," in IEEE International Symposium on the Physical and Failure Analysis of Integrated Circuits, Singapore, 2018.
- [2] H. Villarraga-Gómez, D. Sirny, M. Terada, M. Norouzi Rad, and A. Gu, "Workflows for assessing electronic devices with 3D X-ray microscopy and nanoscale computed tomography," in 12th Conference on Industrial Computed Tomography (iCT), Fürth, Germany, 2023.
- [3] H. Villarraga-Gómez, E. L. Herazo and S. T. Smith, "X-ray computed tomography: from medical imaging to dimensional metrology," *Precision Engineering*, vol. 60, pp. 544-569, 2019.
- [4] C. Jacobsen, *X-ray Microscopy*, New York, NY, USA: Cambridge University Press, 2020.
- [5] H. Toda, *X-Ray CT: Hardware and Software Techniques*, Cham, Switzerland: Springer, 2021.
- [6] H. Villarraga-Gómez, N. Kotwal, N. Parwani, D. Weiß, M. Krenkel, W. Kimmig and C. Graf vom Hagen, "Improving the dimensional accuracy of 3D X-ray microscopy data," *Measurement Science and Technology*, vol. 33, no. 7, p. 074002 (18p), 2022.
- [7] H. Villarraga-Gómez, D. L. Begun, P. Bhattad, K. Mo, M. Norouzi Rad, R. T. White and S. T. Kelly, "Assessing rechargeable batteries with 3D X-ray microscopy, computed tomography, and nanotomography," *Nondestructive Testing and Evaluation*, vol. 37, no. 5, pp. 519-535, 2022.
- [8] A. Tkachuk, F. Diewer, H. Cui, M. Feser, S. Wang and W. Yun, "X-ray computed tomography in Zernike phase contrast mode at 8 keV with 50-nm resolution using Cu rotating anode X-ray source," *Zeitschrift für Kristallographie-Crystalline Materials*, vol. 222, no. 11, pp. 650-655, 2007.
- [9] G. E. Ice, J. D. Budai and J. W. L. Pang, "The race to X-ray microbeam and nanobeam science," *Science*, vol. 334, no. 6060, pp. 1234-1239, 2011.
- [10] E. Maire and P. J. Withers, "Quantitative X-ray tomography," *International Materials Reviews*, vol. 59, no. 1, pp. 1-43, 2014.
- [11] J. Kastner and C. Heinzl, "X-ray Computed Tomography for Non-destructive Testing and Materials Characterization," in *Integrated Imaging and Vision Techniques for Industrial Inspection*, edited by Liu Z, Ukida H, Ramuhalli P, Niel K; London, England (UK), Springer, 2015, pp. 227-250.
- [12] H. Villarraga-Gómez, M. Norouzi Rad, M. Andrew, A. Andreyev, R. Sanapala, L. Omlor and C. Graf vom Hagen, "Improving throughput and image quality of high-resolution 3D X-ray microscopes using deep learning reconstruction techniques," in 11th Conference on Industrial Computed Tomography (iCT), Wels, Austria, 2021.
- [13] A. Gu, M. Terada, H. Stegmann, T. Rodgers, C. Fu and Y. Yang, "From system to package to interconnect: An artificial intelligence powered 3D X-ray imaging solution for semiconductor package structural analysis and correlative microscopic failure analysis," in IEEE International Symposium on the Physical and Failure Analysis of Integrated Circuits (IPFA), Singapore, Singapore, 2022.
- [14] H. Villarraga-Gómez, A. Andreyev, M. Andrew, H. Bale, R. Sanapala, M. Terada, A. Gu, B. Johnson, L. Omlor and C. Graf vom Hagen, "Improving scan time and image quality in 3D X-ray microscopy by deep learning reconstruction techniques," in *Proc. 35th ASPE Annual Meeting*, Vol 75, pp. 361-366, Minneapolis, Minnesota, USA, 2021.
- [15] A. Gu, A. Andreyev, M. Terada, B. Zee, S. Mohammad-Zulkifli and Y. Yang, "Accelerate your 3D X-ray failure analysis by deep learning high resolution reconstruction," in *Proc. 47th International Symposium for Testing and Failure Analysis*, Phoenix, AZ, USA, 5p, 2021.